



The improvement in organic photovoltaic response by inserting an interlayer between MoO₃ and mixed layer of C₆₀:5 wt% TAPC



Xingwu Yan^{a,b}, Wenlian Li^{a,*}, Zisheng Su^{a,*}, Bei Chu^a, Junbo Wang^a, Fangming Jin^{a,b}, Ruigang Li^a, Yuan Gao^{a,b}, Tianyou Zhang^{a,b}, Bo Zhao^{a,b}, Hairuo Wu^{a,b}, Chengyuan Liu^{a,b}, Tong Lin^{a,b}, Qiaogang Song^{a,b}

^a State Key Laboratory of Luminescence and application, Changchun Institute of Optics, Fine Mechanics and Physics, Chinese Academy of Sciences, 3888-Dong Nan Hu Road, Changchun 130033, PR China

^b Graduate School of the Chinese Academy of Sciences, Beijing 100039, PR China

ARTICLE INFO

Article history:

Received 18 November 2014

Received in revised form 21 March 2015

Accepted 27 March 2015

Available online 28 March 2015

Keywords:

SubPc

Interlayer

Built-in field

Spectral response

Bulk heterojunction

ABSTRACT

We demonstrate organic photovoltaic (OPV) cells with structure of ITO/MoO₃ (5 nm)/boron subphthalocyanine chloride (SubPc) (*d* nm)/C₆₀:5 wt% 1,1-bis-(4-methyl-phenyl)-aminophenyl-cyclohexane (TAPC) (40 nm)/BCP (8 nm)/Al, where *d* = 0, 1, 3, 5, 7 and 13 nm. We found that a 5-nm-thick SubPc based cell had a peak power conversion efficiency (PCE) of 3.75% and a voltage (Voc) of 1.03 V, which was an increase of 35.4% and 0.19 V, respectively, compared with the reference cell without SubPc. We found that the spectral response of cells with 1–5 nm SubPc mostly corresponded to the C₆₀ absorption and the cell with 5 nm SubPc had the highest responsivity. The spectral response of the cell with 13 nm SubPc corresponded to both C₆₀ and SubPc absorptions, which is analogous to a previously reported flat heterojunction cell. The excellent PV parameter of the cell with 5 nm SubPc was attributed to a built-in field induced by the Schottky barrier contact of MoO₃/5-nm SubPc. To confirm this hypothesis, another two series of OPV cells with different interlayers and donors instead of SubPc and TAPC were developed.

© 2015 Elsevier B.V. All rights reserved.

1. Introduction

Organic photovoltaic (OPV) cells are potential low-cost alternative renewable sources of energy in comparison with their conventional inorganic counterparts because of their ease of processing and compatibility with flexible substrates. Since 1986, when Tang [1] introduced the donor–acceptor (DA) type OPV cells, PV performance has been continuously improved by designing new PV cell architecture, selecting and synthesizing organic materials. This has helped increase the power conversion efficiency (PCE), which has now reached above 10% for state of the art OPV cells [2,3]. To achieve a highly efficient OPV cell, bulk heterojunction (BHJ) structures using DA co-deposited films have generally been used as active layer [4]. With a few exceptions, [5] fullerenes (C₆₀ and C₇₀) [6,7] have been mostly been used as the acceptor component in small molecule BHJ OPV cells. Simultaneously, many different hole transporting materials have been used as the donor component.

Recently, Tang and co-workers have reported OPV cells with ITO/MoO₃/C₆₀ structure, which had high open circuit voltage

(Voc) of about 1.22 V [8]. Such a high Voc is dependent on a built-in potential residing in the C₆₀ active layer and also on the built-in potential determined by the difference between the work function of MoO₃ and the lowest unoccupied molecular orbital (LUMO) of C₆₀ because of the formation of a Schottky barrier between MoO₃ and C₆₀ [8]. To further improve the PV parameters, this group has addressed a series of cells with 5 wt% of various donors with C₆₀ in a BHJ. The 5 wt% 1,1-bis-(4-methyl-phenyl)aminophenylcyclohexane (TAPC):C₆₀ based OPV cell had a peak PCE of 2.8%. This high PCE could be attributed to the formation of a Schottky junction of MoO₃/BHJ with the C₆₀:TAPC mixed layer [9]. The Holmes group demonstrated an OPV cell with a planar HJ (PHJ) structure using MoO₃/SubPc (boron subphthalocyanine chloride)/C₆₀. The group determined that the MoO₃-SubPc interface can dissociate excitons by measuring the photoluminescence of a 5-nm-thick layer of SubPc with and without an adjacent layer of MoO₃. They concluded that the deeper Fermi level of MoO₃ could cause a large built-in field in the active layer, which may assist with charge collection. This means that the MoO₃-SubPc junction is capable of dissociating excitons and the device had a higher Voc. The Voc originated from the quasi-Fermi level offset at the DA interface and the built-in potential resulted from the Schottky junction [6]. In such a level alignment the loss in the

* Corresponding authors.

E-mail addresses: wliioel@aliyun.com (W. Li), suzs@ciomp.ac.cn (Z. Su).

built-in electric field of the OPV devices can be reduced, leading to an increase in the Voc [10]. The high Voc is determined by the highest occupied molecular orbital (HOMO) of the donor and the LUMO of acceptor [11,12,13], as well as other contributing factors. In Ref. [14], the effect of inserting MoO₃ between the ITO anode and various donors on PV performance was studied. A Voc of 1.05 V and a PCE of 2.9% was achieved for a MoO₃/14-nm SubPc/C₆₀ PHJ cell.

In this manuscript the design of a new OPV cell structure is reported. Our aim was to further improve PV performance. The effect of inserting various organic interlayers between MoO₃ and the BHJ of C₆₀:5 wt% TAPC and of introducing various donors instead of TAPC on the PV parameters was demonstrated. We find that when a SubPc was used as the interlayer, there was a stronger built-in field in the C₆₀:TAPC BHJ. Finally, we fabricated a series of OPV cells in which the thicknesses of MoO₃ and C₆₀:5 wt% TAPC blend layer were 5 and 40 nm, respectively, as well as using various thicknesses of SubPc. We show that a cell with a 5-nm SubPc interlayer had a peak PCE of 3.75% and a maximum Voc of 1.03 V, which were increased by 35.4% and 0.2 V compared with the reference cell without SubPc. When rubrene was used as the interlayer instead of SubPc, the cells had a peak PCE of 3.16%, which was an increase by 13.4% over the reference cell.

The most intense spectral response that corresponded to the C₆₀ absorption was observed by inserting a 5-nm-thick SubPc layer. The rising spectral response that corresponded to the region of the C₆₀ absorption was from the enhanced built-in field in the C₆₀:TAPC BHJ. Thus short current density (Jsc) and PCE improved. The spectral response was different from the OPV with SubPc/C₆₀ PHJ because the external quantum efficiency (EQE) of the cell with 14 nm SubPc as a donor corresponded to both the SubPc and C₆₀ absorptions [14]. To further verify the effect of the SubPc interlayer on the PV parameters, we also determined the influence of various interlayers and donors on PV performance of the two series of cells. These results have also confirmed our earlier conclusion. The improvement mechanism and working processes of our optimized OPV cell are also discussed in more detail.

2. Materials and methods

All devices in this work were fabricated on indium tin oxide (ITO) coated glass substrates. The organic materials for fabrication were purchased and used without further purification. Before the organic films were deposited, the ITO substrates were treated in ultraviolet lamp/ozone for 15 min to remove carbon residue. A deposition rate of 1–2 Å/s was maintained for the organic materials and a rate of 10 Å/s for was used for the Al cathode. A calibrated quartz crystal monitor was used to measure the thickness of each layer. The active area of the devices was about 0.3 × 0.3 cm. Current–voltage (*J*–*V*) characteristics were measured with a programmable source meter (Keithley-2400) in the dark and under AM1.5 solar illumination at an intensity of 100 mW/cm². For the (EQE) measurements, light from Xe and quartz halogen lamps were coupled into a monochromator and their intensities were calibrated with a Si-photodiode. The light incident on the device was chopped and the modulated current signal was detected with a current–voltage and lock-in amplifier. All measurements were carried out at room temperature and under ambient conditions without any protective coatings. The series resistance (Rs) was deduced from the derivative of the slope of the *J*–*V* characteristic curve.

3. Results and discussion

Fig. 1(a) shows the schematic illustration of the OPV structures of the reference cell. Fig. 1(b) shows the structure of the C₆₀:5 wt%

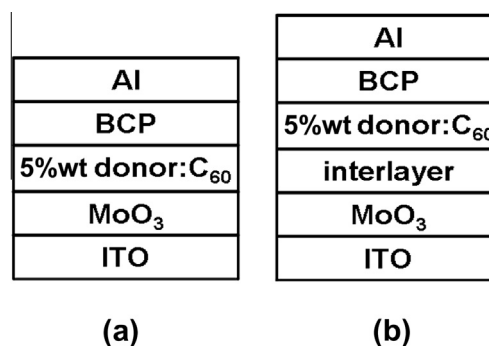


Fig. 1. The schematic illustration of the cell structure for (a) the reference device and (b) the device with different donors using SubPc as the interlayer.

donor cells with different interlayers. Table 1 summarizes the PV performance parameters of a series cells with structure of ITO/MoO₃ (5 nm)/SubPc (*d* nm)/C₆₀:5 wt% TAPC (40 nm)/BCP (5 nm)/Al, where *d* was 0, 1, 3, 5, 7 or 13 nm. Fig. 2(a) shows a plot of the Current density–voltage (*J*–*V*) characteristics of the cells with various thicknesses of the SubPc/(C₆₀:TAPC) BHJ under simulated AM1.5G solar illumination at 100 mW/cm². From Table 1 and Fig. 2(a), the peak PCE of the cell with 5 nm SubPc was 3.75%, which was increased by 34.4% compared with the reference cell. From Table 1, we observed that a maximum Voc of 1.03 V was obtained for the optimized cell, which was higher than the reference cell by 0.2 V. To make the reason for the improved PV response clear, we also studied the *J*–*V* characteristics of several other PHJ cells with a 0-, 1-, 3- or 5-nm-thick SubPc layer (see Fig. 2(b)). Comparing Fig. 2(a) with (b), we find when the SubPc thickness of both two series cells is 0, 1, 3 or 5 nm, the PV response was higher for the BHJ than for the PHJ cells. In particular, both the Jsc and Voc were larger for the BHJ than for PHJ cells with 5 nm of SubPc.

The improvement in OPV parameters of the BHJ with a 5-nm SubPc interlayer could be understood as follows. Because of the Schottky barrier contact of the MoO₃/SubPc junction, the downward band bending of SubPc and the resulting built-in field in the SubPc layer were produced. When the C₆₀:TAPC mixed layer was deposited on the 5-nm SubPc surface, band bending of the C₆₀:TAPC mixed layer could also take place although the bending width should be narrower than 40 nm [15]. This is favorable for hole transfer towards the SubPc/MoO₃ interface [6]. That is, the holes induced by incident light in C₆₀:TAPC mixed layer will be swept to the 5-nm SubPc/MoO₃ layer from C₆₀:TAPC-interface via band bending of the TAPC and SubPc layers and were finally extracted by the ITO anode. The width of the SubPc layer should be 5-nm thick. The band bending of the 5 nm of SubPc and C₆₀:TAPC layers would increase in the built-in field in the BHJ of C₆₀:5 wt% TAPC. By virtue of such a built-in field at the mixed layer, the Voc was observably increased and encouraged electron transport away from the C₆₀:TAPC BHJ and towards the cathode.

Therefore, there are two benefits to our cell with the 5-nm SubPc interlayer: the cell contributes to a higher Voc and also to

Table 1
PV performance parameters of the cells with structure of MoO₃ (5 nm)/SubPc (*d* nm)/C₆₀:5 wt% TAPC (40 nm)/BCP (5 nm)/Al cells with different thicknesses of SubPc (*d* = 0–13 nm).

<i>d</i> (nm)	Jsc (mA/cm ²)	Voc (V)	FF	PCE (%)	Rs (Ohm cm ²)
0	6.07	0.83	0.55	2.77	2.59
1	5.90	0.87	0.46	2.38	3.46
3	5.40	0.91	0.44	2.21	3.92
5	7.70	1.03	0.47	3.75	1.37
7	6.50	1.02	0.46	3.16	1.75
13	5.90	0.90	0.42	2.23	8.06

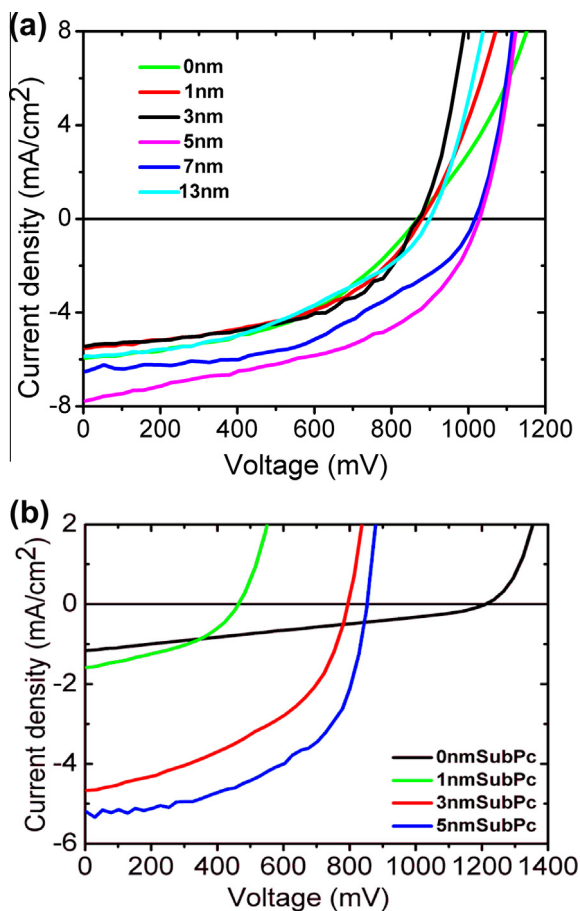


Fig. 2. The current density–voltage characteristics of the OPV cells with (a) MoO₃ (5 nm)/SubPc (*d* nm) C₆₀:5 wt% TAPC (40 nm) (*d* = 0–13 nm) and (b) MoO₃/SubPc (*x* nm) C₆₀ without TAPC (*x* = 0, 1, 3 and 5 nm) under simulated AM1.5G solar illumination at 100 mW/cm².

a lower series resistance and thus a higher PCE was achieved (see Table 1). In this case the lower hole mobility of SubPc [16] could be ignored because of the band bending in both SubPc layer and the mixed layer of C₆₀:5 wt% TAPC. The C₆₀:5 wt% TAPC mixed layer has a higher electron mobility of $4.19 \times 10^{-3} \text{ cm}^2 \text{ V}^{-1} \text{ s}^{-1}$ [9] and so balanced carrier transport and collection by the two electrodes can be realized. In this case, the carrier recombination during carrier transport processes would be reduced, leading to lower series resistances of the cells with 5 nm SubPc compared with cells with other thicknesses of SubPc (see Table 1).

The total Voc is larger than the limit set solely by the energy level difference between the LUMO of C₆₀ and the HOMO of TAPC [9,17] because the Voc of conventional BHJ cells is established by the built-in potential governed by the HOMO/HOMO difference of the donor and acceptor [18]. It was confirmed that in the BHJ cell with 5 nm SubPc, the exciton dissociation was a result of the offset between the HOMO of C₆₀ and the HOMO of TAPC because there was a more appropriate level alignment for exciton dissociation [17].

To further understand the high PCE of the optimized OPV cell, the difference between the PV parameters of the BHJ and PHJ cells with the identical thickness SubPc layers was compared. Firstly, the spectral responses (EQE spectra) of the two series of cells were determined, as shown in Fig. 3(b) and (c). Seeing Fig. 3(a–c), the main difference between the BHJ and PHJ series cells is that: (1) the spectral response in the region of the C₆₀ absorption (350–550 nm) is higher the BHJ cell than for the PHJ cells with

5-nm SubPc layer. The spectral response of the BHJ cell only corresponds to one band in the 350–550-nm region but there were two spectral bands in the PHJ response in the 350–550-nm and 525–600-nm regions; (2) The spectral response of the BHJ and PHJ cells with 1 nm SubPc have an almost identical response that corresponds to the C₆₀ absorption of 350–550 nm but the spectral responsivity is higher for the BHJ cell than for PHJ cells; (3) The responsivity corresponding to the C₆₀ absorption was gradually enhanced with increasing SubPc thickness from 1 to 5 nm. The maximum value was obtained with the 5-nm-thick SubPc; (4) The two spectral responsivities corresponding to the C₆₀ and SubPc absorptions in the BHJ cell with 13 nm of SubPc were almost identical. As shown in Table 1, the cell with 5 nm SubPc had a peak Jsc of 7.70 A/cm², which can be attributed to the maximum spectral response among the cells with different thicknesses (see Fig. 3(b)).

The difference between the OPV performance of BHJ and PHJ cells can be explained as follows. The interface between SubPc/C₆₀ planar HJ offers a smaller contact area compared with the C₆₀:TAPC BHJ. Also, the 5-nm SubPc based BHJ cell does not have spectral response that can be attributed to the SubPc absorption because it is too thin compared with the 40-nm-thick C₆₀:TAPC mixed layer. In the C₆₀:5 wt% TAPC mixed layer there is a sufficiently large contact of donor and acceptor materials, so there is a higher exciton dissociation probability than the PHJ cells [19].

It is interesting that the series resistance (Rs) of the optimized cells is even smaller than that of reference cell (see Table 1). However when the SubPc thickness was further increased to 13 nm, the Rs increased to 8.06 Ω cm² (see Table 1), which leads to a lower fill factor (FF) of 0.42. This cell is similar to the previously reported PHJ cell of MoO₃/14 nm of SubPc/C₆₀ [6,14,20,21]. Thus we could also conclude that when the SubPc thickness is very large, the built-in field induced by the MoO₃/SubPc (13 nm) junction in the C₆₀:TAPC BHJ would weaken because the relative spectral response corresponding to the C₆₀ absorption considerably decreased (see Fig. 3(b)). The SubPc/C₆₀ interface can also dissociate excitons (see Fig. 3(b)). Thus, in this case, the Voc of the device with 13 nm SubPc is mainly dependent on the difference between the LUMO of SubPc and the HOMO of C₆₀. However, the built-in field could provide a smaller contribution to the increase of the Voc compared with cells with 5 nm SubPc because the thick SubPc layer would lead to narrower band bending region of SubPc.

The HOMO and LUMO levels of the interlayer and other materials used in this study are displayed in Fig. 4.

To verify the presence of an intense built-in field in the C₆₀:TAPC BHJ in cell with 5 nm SubPc, the effect of another 5 nm several interlayers such as 4,4-bis[N-(1-naphthyl)-N-phenyl-amino]biphenyl (NPB) and rubrene, copper-phthalocyanine (CuPc), 4,4'-N,N'-dicarbazole-biphenyl (CBP) and 4,4,4-tris(N-carbazolyl)triphenyl amine (TCTA) on the PV parameters was also investigated as shown in Fig. 5(a) and Table 2. It can be seen that except for the SubPc-based cell, the CuPc-based cell has a lower PCE of 1.02%, which is almost identical to that of MoO₃/CuPc/neat C₆₀ PHJ cell (see Ref. [10]). The reason that why CuPc-based cell has a low PCE may be because of the lack of the built-in potential at the CuPc layer because of its shallower HOMO level compared with SubPc (see Fig. 4) [6]. The NPB-interlayer cell has a low PCE of 1.49%, which may be attributed to the presence of weaker built-in field at the C₆₀:TAPC layer because its spectral response at 350–550 nm is even lower than that of the reference cell (Fig. 5(b)). We have also observed lower PV response of the TCTA- and CBP-based cells because their Vocs are lower than the SubPc cell. We note that the HOMO levels of both TCTA and CBP are deeper than SubPc (see Fig. 4). This would lead to the difficulty in transporting of holes that were derived from C₆₀:TAPC BHJ

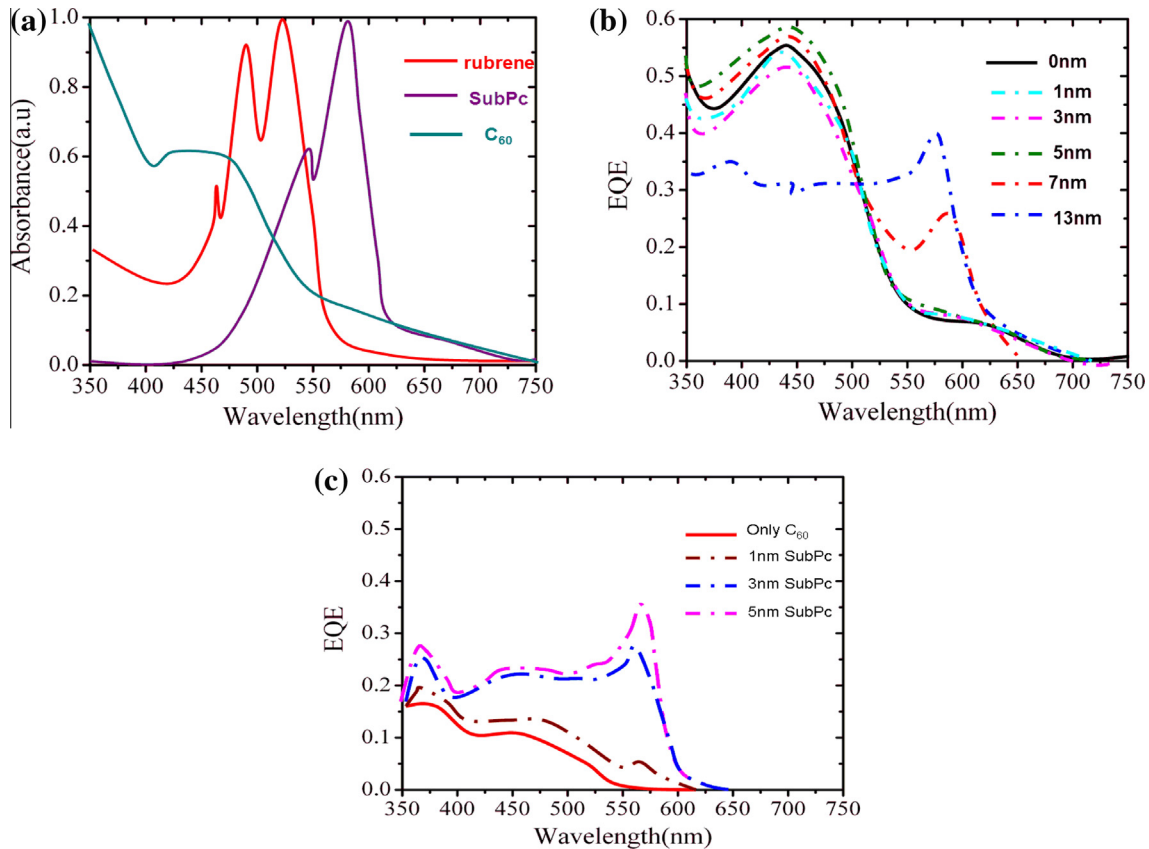


Fig. 3. (a) The absorption spectra of SubPc, rubrene, and neat C₆₀ films (b) the external quantum efficiency (EQE) of OPV cells with different thicknesses of SubPc and (c) OPV with PHJ of MoO₃/SubPc (0–5 nm)/C₆₀.

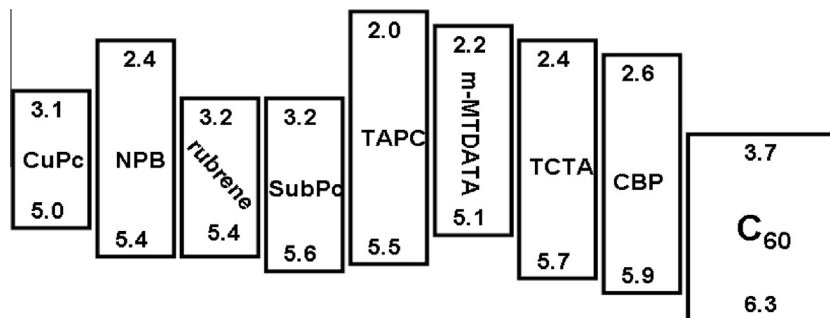


Fig. 4. The LUMO/HOMO levels of the various donors. The interlayer values were taken from literature: CuPc and C₆₀ values were taken from Ref. [13], CBP and TCTA were taken from Ref. [20], NPB, and the TAPC values were taken from Ref. [22]. Rubrene and (m-MTDATA) were taken from Refs. [23,24], respectively.

because there would be a barrier for hole transport via the HOMO level of TCTA or CBP towards MoO₃/ITO. Rubrene-based cells had a higher PCE of 3.12%, which is close to that reported in Ref. [23], in which anode buffer is poly(ethylenedioxythiophene):poly(styrene sulphonic acid) (PEDOT:PSS) which has a higher work function. The PEDOT:PSS/rubrene junction should be similar to a Schottky junction and hence a higher V_{oc} of 0.91 V was achieved. Therefore, in this case, there would also be a stronger built-in field in the C₆₀:TAPC mixed layer because the spectral response at 350–550 nm almost the same as the 5-nm SubPc cell (see Fig. 5(c)).

It was shown that the 5-nm SubPc interlayer between MoO₃ and mixed layer of C₆₀:TAPC plays a crucial role in the improvement of the PV performance. To further confirm the contribution of 5 nm SubPc to the performance improvement, we also designed another a series of cells with a different 5 wt% donor:C₆₀. 4,4',4''-tris[N, (3-methylphenyl)]-N-phenylamino]-triphenylamine

(m-MTDATA), TCTA and CBP were used as the donors and their LUMO/HOMO levels are shown in Fig. 4. The PV parameters of these cells are listed in Table 3. When these donors were incorporated instead of TAPC, the PCE was enhanced by 71.8% when m-MTDATA was used, by 50% when TCTA was used and by 34.9% when CBP was used compared with their respective reference cells. The V_{oc}s of these cells also increased over the reference cell. The V_{oc} of the m-MTDATA-cell also increased because the difference between the HOMO of m-MTDATA and the LUMO of C₆₀ was small [17]. The PV response of cells using several donors was lower than the TAPC-based cell. This was attributed to the inappropriate level alignment of the HOMO of C₆₀ and the HOMO of the donor for exciton dissociation (see Fig. 5) [17]. Even so, such an enhancement effect is also significant for the design of new OPV structures.

In summary, under illumination, the MoO₃/SubPc Schottky junction led to band bending of SubPc. The lowered HOMO level

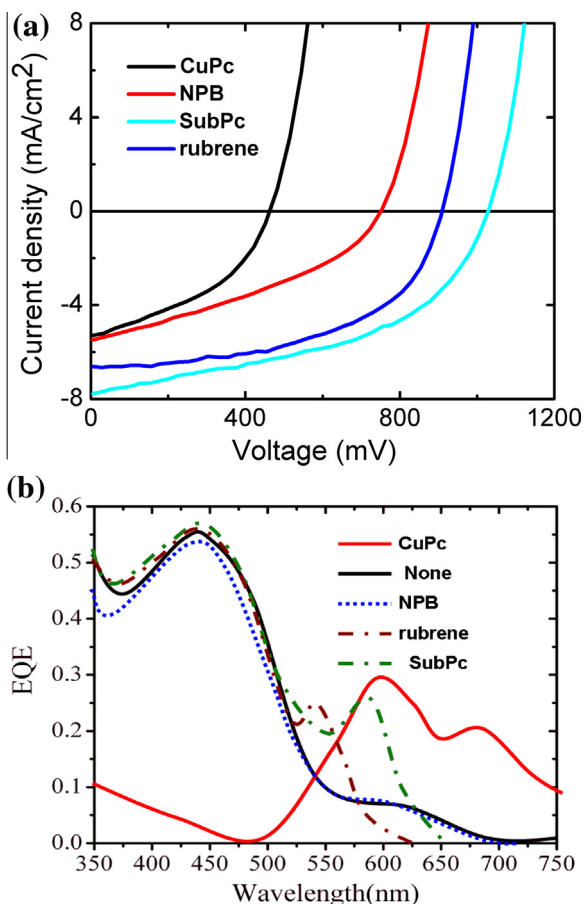


Fig. 5. (a) Current density–voltage characteristics for OPV cells with 5 nm different interlayers under simulated AM1.5G solar illumination at 100 mW/cm² and (b) the EQE of the OPV cell with different interlayers keeping the mixed 5 wt.% TAPC:C₆₀ (40 nm) constant.

Table 2
PV parameters of cells with different interlayers when keeping the 5 wt.% TAPC doping C₆₀ matrix constant.

Interlayer (5 nm)	J _{sc} (mA/cm ²)	V _{oc} (V)	FF	PCE (%)
CuPc	5.3	0.47	0.42	1.02
NPB	5.5	0.73	0.35	1.49
SubPc	7.7	1.03	0.47	3.75
Rubrene	6.6	0.91	0.53	3.12
CBP	3.6	0.72	0.47	1.22
TCTA	4.2	0.79	0.46	1.53

Table 3
PV response of the cells with C₆₀:5 wt% with different donors in the C₆₀ matrix with a 7-nm-thick SubPc interlayer.

Donor material	J _{sc} (mA/cm ²)	V _{oc} (V)	FF	PCE (%)
TCTA	5.50	1.07	0.32	1.89
Without SubPc	3.01	0.99	0.37	1.1
CBP	3.00	1.21	0.29	1.05
Without SubPc	2.17	1.10	0.27	0.7
m-MTDATA	3.59	0.88	0.37	1.16
Without SubPc	2.30	0.80	0.46	0.86

of SubPc would assist with free hole transport from the C₆₀:TAPC BHJ to the anode via the bended SubPc HOMO level. There was also a stronger built-in field in the mixed layer of C₆₀:5 wt% TAPC after the mixed layer was deposited on the 5-nm SubPc layer. Thus, the total Voc was equal to sum of the Voc resulting from band gap of

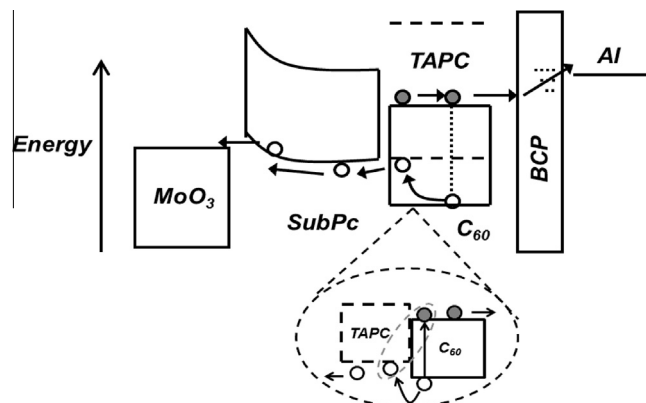


Fig. 6. Schematic working processes and detailed operating mechanism of the optimal PV cell with 5 nm SubPc. The small bottom figure shows the exciton dissociation process at the C₆₀:TAPC BHJ interface. (Circles denote light generated electrons (black) and holes (white).)

the HOMO of TAPC and the LUMO of C₆₀ and a contribution from the built-in field residing at the C₆₀:TAPC BHJ.

The appropriate level offset (0.8 eV) between the HOMO of C₆₀ and the HOMO of TAPC would increase the probability of exciton dissociation [17]. The free electrons and holes originating from the C₆₀:TAPC BHJ would easily be transported towards the cathode via the LUMO of C₆₀ and to the ITO via bending of the HOMO level of SubPc, respectively. The energy level alignment, schematic band-bending and detailed device operation of the optimized cell are shown in Fig. 6.

4. Conclusion

We demonstrated the PV performance of OPVs using different SubPc interlayer thicknesses. We observed that the cell with 5 nm of SubPc had the maximum Voc and PCE. The improvement in the PV response was attributed to the MoO₃/SubPc Schottky junction, which lead to the band bending of the SubPc layer. This assists with free hole transport from the C₆₀:TAPC BHJ to the anode via band bending of the SubPc HOMO. After the C₆₀:TAPC mixed layer was deposited on the SubPc layer, band bending of C₆₀:TAPC mixed layer also took place so that there was a stronger built-in field in the mixed layer. Thus, the Voc should originate from the sum of the band gap between the HOMO of TAPC and the LUMO of C₆₀ and from the contribution of the built-in field. The improvement in the PV parameters by inserting 5 nm SubPc between MoO₃ and C₆₀:5 wt% TAPC was also supported by results of another two series of cells. This new finding will guide better design and selection of new organic electronic devices and materials. The findings are significant because a thinner SubPc layer and a spectral response that only contains a contribution from the C₆₀ absorption could be used for designing a tandem cell and other electronic devices. More detailed studies will be submitted elsewhere.

Acknowledgments

This work was supported by the National Natural Science Foundation of China (61107082, 61376022 and 61376062) and the Science and Technology Development Plan of Jilin Province (20110321).

References

- [1] C.W. Tang, *Appl. Phys. Lett.* 48 (1986) 183.
- [2] Z.C. He, C.M. Zhong, S.J. Su, M. Xu, H.B. Wu, Y. Cao, *Nat. Photonics* 190 (2012) 1.

- [3] Z.C. He, C.M. Zhong, X. Huang, W.Y. Wong, H.B. Wu, L.W. Chen, S.J. Su, Y. Cao, *Adv. Mater.* 23 (2011) 4636.
- [4] A.K. Pandey, S. Dabos-Seignon, J.M. Nunzi, *Appl. Phys. Lett.* 89 (2006) 113506.
- [5] N. Beaumont, S.W. Cho, P. Sullivan, D. Newby, K.E. Smith, T.S. Jones, *Adv. Mater.* 22 (2012) 561.
- [6] Y. Zou, R.J. Holmes, *Appl. Phys. Lett.* 103 (2013) 053302.
- [7] G. Chen, H. Sasabe, Z.Q. Wang, X.F. Wang, Z.R. Hong, Y. Yang, J. Kido, *Adv. Mater.* 24 (2012) 2768.
- [8] M. Zhang, Irfan, H.J. Ding, Y.L. Gao, C.W. Tang, *Appl. Phys. Lett.* 96 (2010) 183301.
- [9] M.L. Zhang, H. Wang, H.K. Tian, Y.H. Geng, C.W. Tang, *Adv. Mater.* 23 (2011) 4960.
- [10] I. Hancox, P. Sullivan, K.V. Chauhan, N. Beaumont, L.A. Rochford, R.A. Hatton, T.S. Jones, *Org. Electron.* 11 (2010) 2019.
- [11] P. Rand, J. Xue, S. Uchida, S.R. Forrest, *J. Appl. Phys.* 98 (2005) 124902.
- [12] S.W. Cho, L.F.J. Piper, A. DeMasi, A.R.H. Preston, K.E. Smith, K.V. Chauhan, P. Sullivan, R.A. Hatton, T.S. Jones, *J. Phys. Chem. C* 114 (2010) 1928.
- [13] K. Schulze, C. Uhrich, R. Schuppel, K. Leo, M. Pfeiffer, E. Brier, E. Reinold, P. Bauerle, *Adv. Mater.* 18 (2006) 2872.
- [14] I. Hancox, P. Sullivan, K.V. Chauhan, N. Beaumont, L.A. Rochford, R.A. Hatton, T.S. Jones, *Org. Electron.* 11 (2010) 188.
- [15] X.L. Liu, S.J. Yi, C.G. Wang, C.C. Wang, Y.L. Gao, *J. Appl. Phys.* 115 (2014) 163708.
- [16] P. Heremans, D. Cheyons, B.P. Rand, *Acc. Chem. Res.* 42 (2009) 1740.
- [17] F.M. Jin, B. Chu, Z.S. Su, B. Zhao, T.Y. Zhang, X.W. Yan, Y. Gao, H.R. Wu, C.S. Lee, J.Z. Zhu, H.C. Pi, J.B. Wang, *Organic Electron.* 14 (2013) 1130.
- [18] C.J. Brabec, A. Cravino, D. Meissner, N.S. Sariciftci, T. Fromherz, M.T. Rispens, L. Sanchez, J.C. Hummelen, *Adv. Funct. Mater.* 11 (2001) 374.
- [19] K. Vandewal, J. Widmer, T. Heumueller, C.J. Brabec, M.D. McGehee, K. Leo, M. Riede, A. Salleo, *Adv. Mater.* 26 (2014) 3839.
- [20] R. Pandey, Y. Zou, R.J. Holmes, *Appl. Phys. Lett.* 101 (2012) 033308.
- [21] R. Pandey, A.A. Gunawan, K.A. Mkhoyan, R.J. Holmes, *Adv. Funct. Mater.* 22 (2012) 615.
- [22] S.H. Kim, J. Jang, J.Y. Lee, *Appl. Phys. Lett.* 91 (2007) 083511.
- [23] C. Kulshreshtha, J.W. Choi, J.K. Kim, W.S. Jeon, M.C. Suh, Y.S. Park, J.H. Kwon, *Appl. Phys. Lett.* 99 (2011) 023308.
- [24] T. Taima, J. Sakai, T. Yamanari, K. Saito, *Jpn. J. Appl. Phys.* 45 (2006) L995.